EXTENDED SEMI-ANALYTICAL MODEL FOR THE PREDICTION OF FLOW AND CONCENTRATION FIELDS IN A TANGENTIALLY-FIRED FURNACE

by

Amin LOTFIANI* * and Shahram KHALILARYA

Mechanical Engineering Department, Urmia University, Urmia, Iran

Original scientific paper
DOI: 10.2298/TSCI121117127L

Tangentially-fired furnaces are one of the modified types of furnaces which have become more attractive in the field of industrial firing systems in recent years. Multi-zone thermodynamic models can be used to study the effect of different parameters on the operation of tangentially-fired furnaces readily and economically. Flow and mixing sub-model is a necessity in multi-zone models. In the present work, the semi-analytical model previously established by the authors for the prediction of the behavior of coaxial turbulent gaseous jets is extended to be used in a single-chamber tangentially-fired furnaces with square horizontal cross-sections and to form the flow and mixing sub-model of the future multi-zone model for the simulation of this tangentially-fired furnaces. A computer program is developed to implement the new extended model. Computational fluid dynamics simulations are carried out to validate the results of the new model. In order to verify the computational fluid dynamics solution procedure, a turbulent round jet injected into cross flow is simulated. The calculated jet trajectory and velocity profile are compared with other experimental and numerical data and good agreement is observed. Results show that the present model can provide very fast and reasonable predictions of the flow and concentration fields in the tangentially-fired furnaces of interest.

Key words: *tangentially-fired furnace, semi-analytical model, multi-zone model, turbulent mixing, diffusion combustion, computational fluid dynamics*

Introduction

In most industrial combustion and flame applications, the achievement of high heat transfer rates and low pollutant emissions using diffusion furnaces is a target and is desirable. Uniform heat flux in industrial furnaces is of great importance because local overheating and high thermal stresses result in components failure and shorter furnace lifetime. Taking account of different parameters, engineers have continuously modified furnaces to meet the above-mentioned requirements. Tangentially-fired furnaces (TFF) are one of the modified types of furnaces which have become more attractive in the field of industrial firing systems such as power station boiler furnaces in the last years. In these furnaces, several coaxial fuel-air jets are directed at an imaginary circle in the middle of the furnace to bring about a vortex motion. Each coaxial jet impinges upon the adjacent jet and deflects it. Thus the initially-free coaxial fuel-air jets no longer remain free after the impingement. Some recent works on TFF are introduced below.

Vagner [1] experimentally studied a tangentially-fired co-generation plant boiler in order to raise its thermal efficiency and to reduce the harmful emissions. Habib *et al*. [2] numeri-

* Corresponding author; e-mail: amn622002@yahoo.com

cally studied the flow field and thermal characteristics in a model of a tangentially-fired furnace under different conditions of burner tripping. Belosevic *et al*. [3] presented numerical simulations of processes in a tangentially-fired utility boiler furnace and performed measurements to validate their numerical results. Diez *et al.* [4] numerically investigated NO_x emissions from a tangentially fired utility boiler under conventional and overfire air operating conditions. They validated the results against actual measurements. Li *et al*. [5] performed full-scale experiments on a 300 MW_e tangentially fired utility boiler retrofitted with air staging. Zhou *et al.* [6] studied the flow field in upper furnace of large-scale tangentially-fired boilers numerically and experimentally. Modlinski [7] numerically investigated a utility boiler TFF using 3-D CFD simulations. The traditional jet burners were replaced with rapid ignition swirl burners to enhance the furnace performance.

Most of the numerical data available on TFF are obtained from CFD solutions which are considerably easier and faster than physical experiments and field measurements. However, in comparison with thermodynamic models, they are time-consuming, computationally expensive, and even problematic in large TFF because of the increased grid sizes. Thermodynamic models, including zero-dimensional single-zone and quasi-dimensional multi-zone models, can be used to study the effect of different parameters on the operation of TFF in an economical and easy way. Flow and mixing sub-model is a necessity in multi-zone models. In the present work, the semi-analytical model previously established by the authors for the prediction of the behavior of coaxial turbulent gaseous jets [8] is extended to be used in a single-chamber TFF with square horizontal cross-sections and to form the flow and mixing sub-model of the future multi-zone model for the simulation of this TFF. Results are compared with other experimental and numerical data and good agreement is observed.

Problem specifications

In the semi-analytical model previously developed by the authors [8], simple relations were proposed to predict the flow and concentration fields of coaxial turbulent gaseous jets. These relations were applicable to all the regions of the jets. It was demonstrated that the model was very fast compared to CFD solution and could provide reasonably accurate predictions. However the model could be used only for axisymmetric furnaces. In the present work, this model is extended to be used in a single-chamber TFF with square horizontal cross-sections.

Fuel and air are admitted into the combustion chamber in a tangential manner from its sides. Fuel enters the combustion chamber from a round nozzle and air is admitted through an annulus surrounding the central fuel nozzle. Four coaxial fuel-air jets are directed at an imaginary circle in the middle of the furnace. Each of the coaxial jets impinges upon the adjacent jet and deflects it. Thus the initially-free coaxial fuel-air jets no longer remain free after the impingement. In addition, impingement of the coaxial jets brings about a vortex motion in the middle of the furnace. This vortex entrains lean and rich zones and blends them together for efficient mixing and combustion [2, 9, 10]. Therefore it is necessary to study the interaction of the coaxial jets and also the effect of the vortex on the velocity and concentration fields, before extending the previously-developed model.

To carry out this study and to perform the procedure mentioned above, part of a TFF is simulated, under isothermal conditions. This part is 150 mm high and the burners are accommodated midway between its top and bottom faces. The opposite burners are adjusted to be 50 mm apart laterally, to create the vortex in the middle of the furnace. This equals the diameter of the imaginary circle. Each burner consists of two coaxial pipes. The inner pipe diameter (round fuel nozzle) is 10 mm and the outer pipe diameter (larger diameter of the annular air passage) is 30 mm.

The side length of the furnace square cross-section is 560 mm. Operating pressure is 101325 Pa and the temperature is 300 K. Geometry and dimensions of the furnace, arrangement of the burners, and details of the coaxial nozzles are shown in fig. 1.

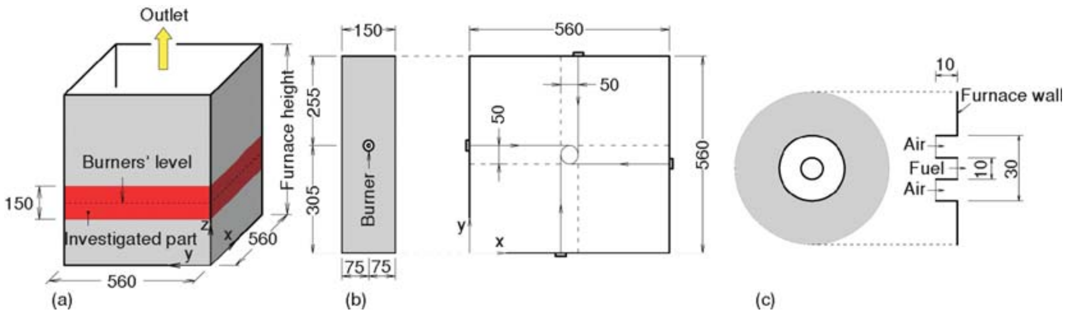

Figure 1. (a) Geometry and dimensions (in mm) of the furnace chamber; (b) Arrangement of the burners; (c) Details of the coaxial nozzles

Physical processes in TFF

Two main physical processes take place in TFF: the vortex-aided mixture formation and the interaction of the coaxial fuel-air jets. As mentioned before, each of the four coaxial fuel-air jets impinges upon the adjacent jet and deflects it. This creates a large vortex in the middle of the furnace, which provides rapid contact between fuel and air, entrains lean and rich zones and blends them together. The vortex ensures an efficient mixing of fuel with air and, in turn, a reliable combustion with uniform temperature distribution [2, 9, 10]. Also, slugging of the furnace walls, erosion, and local over-heating are prevented or minimized by the central vortex mentioned. Therefore, the effect of the central vortex on the flow and concentration fields should be taken into account.

The initially-free coaxial fuel-air jets no longer remain free after they impinge upon each other and deflect. It is necessary to study the interaction of the jets and to determine the trajectory of the deflected coaxial jets for the purpose of developing the desired new model. The same definition of jet trajectory is used as was used by Kamotani and Greber [11]. Jet trajectory is the locus of the maximum velocity in the plane of symmetry. With the assumption that the trajectory of a round fuel jet in the flow field of TFF is only a function of the jet fluid density ρ_f and viscosity μ_f, velocity at the nozzle exit v_f, nozzle diameter d_1, and the side length of the furnace square cross-section L, dimensional analysis yields:

$$\frac{x}{L}=\mathrm{f}_1\left(\frac{y}{L},\frac{\rho_f v_f d_1}{\mu_f}\right)=\mathrm{f}_1\left(\frac{y}{L},\mathrm{Re}\right) \tag{1}$$

In this equation, x and y are the co-ordinates as shown in fig. 1.

Taking account of the air jet which is admitted into the combustion chamber through the annular passage around the central fuel nozzle, additional parameters such as air density ρ_a and viscosity μ_a, velocity at the exit of the annular air nozzle v_a, and the larger diameter of the annular air passage d_2 must be included in the analysis. In this case, dimensionless groups MR and μ_a/μ_f are added to those in eq. (1). MR is the momentum ratio, *i. e.* the ratio of the annular jet momentum to the round jet momentum. Since high Reynolds numbers are used in most of the practical combustion systems, the ratio of inertial forces to viscous forces is high and it is reasonable to neglect the effect of μ_a/μ_f on the jet trajectory compared to the other dimensionless groups. Therefore,

$$\frac{x}{L} = f_2\left(\frac{y}{L}, \text{Re}, MR\right) \tag{2}$$

In subsequent sections, 3-D CFD simulations will be made to find out how Re and *MR* affect the trajectory of the coaxial fuel-air jets in the flow field of TFF.

The new extended model

Once the trajectory of the coaxial fuel-air jets in the flow field of TFF is determined, velocity and concentration fields can be obtained using the previously-developed model for the prediction of the behavior of coaxial turbulent gaseous jets. Calculations are performed only in one quarter of the combustion chamber because of the rotationally-repetitive nature of the flow in TFF. Velocities and concentrations in the three remaining quarters of the furnace are found by rotating the calculated fields in the first quarter. The effect of the vortex motion at the furnace center on the flow and concentration fields is taken into account via corrections to them.

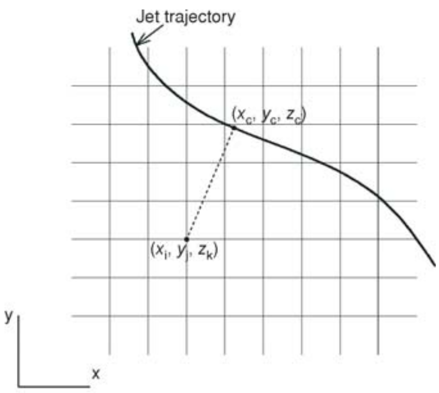

Figure 2. Determination of the point on the jet centerline corresponding to the desired point where velocity and concentration values must be found

As demonstrated in fig. 2, to determine the velocity and concentration values at any desired point (x_i, y_j, z_k), the corresponding point on the centerline of the deflected jet (x_c, y_c, z_c) must be found. Here, i, j, and k are the running indices in the x, y, and z-directions, respectively. It is assumed that the centerline of the deflected jet lies in a horizontal plane at the burners' level, *i. e.* $z_c = z_b$ [9]. The line connecting the two points mentioned above is perpendicular to the jet centerline. Hence the point on the centerline can be found.

Having determined the point on the jet centerline, the length of the jet trajectory (the centerline of the deflected jet) from the fuel nozzle exit to (x_c, y_c, z_c) is calculated. Trapezoid integration is employed to that end. Significant computational time is saved by computing the integrals up to some different end-points once, storing them in a look-up table, and retrieving them during the main solution. In the main solution, linear interpolation easily provides the integral value of interest.

It is assumed that the velocity and concentration values at (x_c, y_c, z_c) are the same as those on the symmetry axis of the free coaxial fuel-air jets (before deflection) at a distance equal to the length of the deflected jet trajectory up to (x_c, y_c, z_c) from the fuel nozzle exit. Prior to the main solution, velocity, concentration, and other required data are calculated at some arbitrary points along the symmetry axis of the free coaxial jets from the previously-developed model equations and the results are stored in a look-up table for later interpolation in the main solution. Knowing the distance between the points (x_i, y_j, z_k) and (x_c, y_c, z_c), velocity and concentration at (x_i, y_j, z_k) can be obtained from the previous work [8]. The resulting velocity at (x_i, y_j, z_k) is resolved into two components in the x and y directions. Since the *z*-velocity distribution plays only a minor role in the simulation of TFF [2, 3, 6], it is assumed to be uniform at any horizontal cross-section of the combustion chamber. The horizontal plane at the burners' level divides the furnace chamber into the upper and lower parts. It is assumed that the *z*-velocity component in the lower part is zero. This is justified on the grounds that the gases flowing downwards eventually impinge on the furnace floor and return in the opposite direction. Being equal and in opposite directions, the vertical velocity components in the lower part of the combustion chamber cancel each other out. Therefore, it is sufficient to calculate the z-velocity component only in the upper part of the chamber from the continuity equation. When the velocity and concentration fields are determined this way, they should be corrected to take account of the effect of the central vortex on them. The corrections will be indicated in next sections.

CFD calculations

In order to validate the results of the new model, two sets of CFD simulations are made under isothermal conditions, using the flow solver Fluent 6.2. In the first set, the species transport model and in the second, the conserved scalar model is used. In the species transport model, transport equations for the chemical species are solved in addition to the continuity, momentum, and the turbulence model equations for incompressible flow. In the conserved scalar model, species transport equations are not solved. Instead, a transport equation for the mixture fraction is solved and individual species concentrations are derived from the predicted mixture fraction distribution. Turbulence effects are accounted for with the help of an assumed shape probability density function (PDF). The average of the results obtained from the two sets of the simulations is supposed to be representative of the CFD solution. More details about the equations are given in [2, 6, 12].

The turbulence model used is the two-equation Realizable k-ε model. This model is the most suitable one among the two-equation eddy viscosity turbulence models for the simulation of jets and flows involving rotation, re-circulation and strong streamline curvature [7, 9, 12].

All the governing equations are discretized using the second order upwind scheme. The discretized equations are solved using the Simple algorithm. The implicit and segregated solver is applied for the solution of the system of governing equations. The software Gambit 2.2 is employed to generate the geometry and mesh for the computational domain. Computations are performed on three progressively finer meshes to secure grid independence. Results are virtually identical for the three meshes and the minor grid dependence of the results are safely neglected. The chosen mesh consists of 59833 high-quality cells. Most of the cells are hexahedral and a few are tetrahedral/hybrid. To capture the details of the flow accurately, the size of the cells is significantly reduced near the nozzles and the furnace center where large gradients are expected. This 3-D mesh is demonstrated in fig. 3. It can be seen that only one quarter of the whole geometry is meshed.

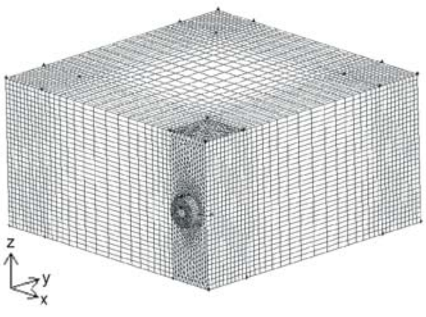

Figure 3. The high-quality 3-D mesh consisting of 59833 cells

Velocity inlet boundaries are used at the fuel and air inlets and pressure outlet boundary is used at the top and bottom faces of the investigated part. Wall boundary with constant temperature of 300 K and no slip condition is used at the chamber walls. Turbulence intensity is assumed to be 5% at the fuel and air inlets and also at the top and bottom faces. Convergence criterion for all the governing equations is the residual value. Solution is considered to be converged when the residual values become less than 10^{-5}. It takes about 10 hours for each solution to converge.

Results and discussion

A turbulent round jet injected into cross flow is simulated to verify the CFD solution procedure because it is a characteristic feature of the flow in TFF. The calculated jet trajectory is compared with the experimental data of Kamotani and Greber [11]. The experimental data of Crabb *et al.* [13] and the large eddy simulation (LES) of Majander and Siikonen [14] are used to evaluate the velocity profile. Good agreement demonstrates the validity of the CFD simulations. Figure 4(a) shows the trajectory of the turbulent round jet in cross-flow. The origin of co-ordinates is placed at the center of the nozzle exit. The x-axis is taken in the cross-flow direction and the z-axis is the centerline of the round nozzle. The ratio of the jet momentum to that of the cross-flow is $J = 32$ and $y = 0$ denotes the symmetry plane of the deflected jet. The jet and cross-flow fluid is air. The x velocity distribution at $y = 0$ and $x/D = 6$ is shown in fig. 4(b). Here, D is the round nozzle diameter, U is the x-velocity component, and U_{cf} is the uniform cross-flow velocity. It can be seen that the results of the present CFD simulations compare favorably with the available experimental and numerical data.

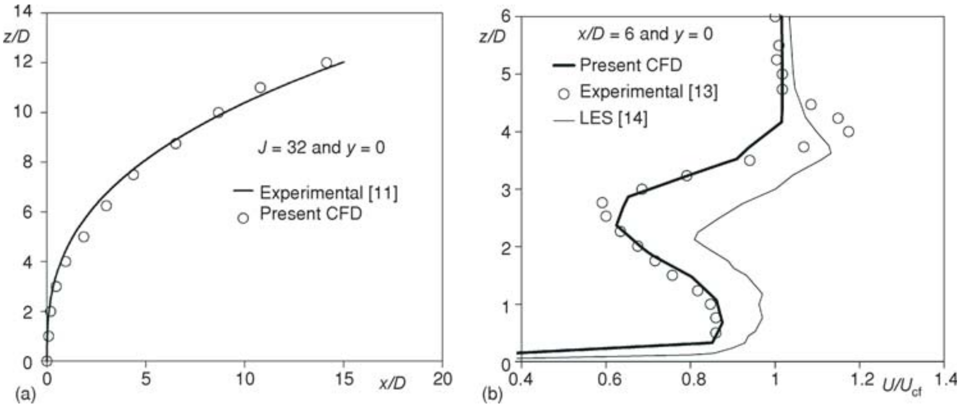

Figure 4. Validation of the present CFD simulations: (a) The trajectory of the turbulent round jet in cross-flow; (b) Distribution of the x-velocity at $y = 0$ and $x/D = 6$

Samples of the flow pattern in TFF with square horizontal cross-sections are shown in fig. 5. Contours of velocity magnitude (in m/s) at the burners' level corresponding to the TFF of the present study with Re = 32888 and $MR = 1.5$ are shown in fig. 5(a). In addition, the flow pattern in two previously-simulated TFF burning methane is indicated in figs. 5(b) and 5(c). More details about these two furnaces are given in [9, 10]. It can be seen that each of the four coaxial jets impinges upon the adjacent jet and deflects it. This creates the vortex in the middle of the furnace. Velocity vectors in fig. 5(c) clearly show the large central vortex and the deflection of the coaxial jets.

Figure 6 demonstrates how Re and *MR* affect the trajectory of the coaxial fuel-air jets in the flow field of TFF with square horizontal cross-sections. The trajectories at different Reynolds numbers and different momentum ratios are shown in figs. 6(a) and 6(b), respectively. The trajectory of the coaxial jets is studied only in one quarter of the furnace because of the rotationally-repetitive flow pattern in TFF. It can be observed that neither of the above-mentioned parameters has influence on the jet trajectory.

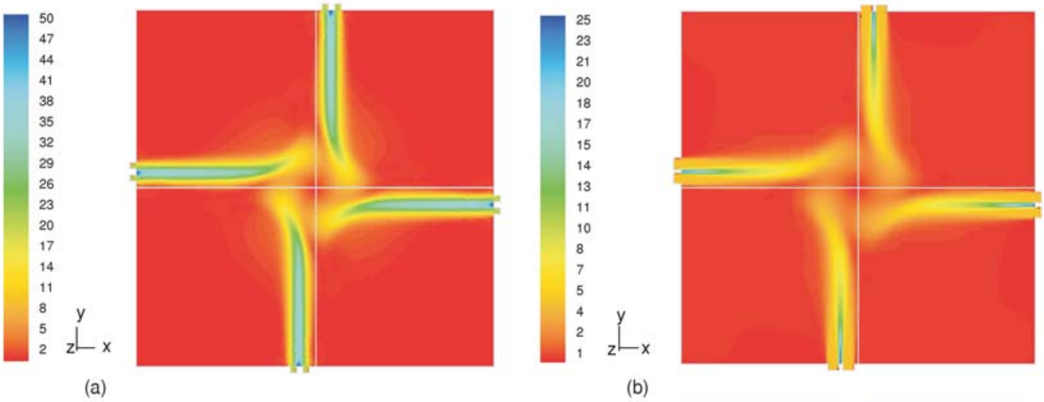

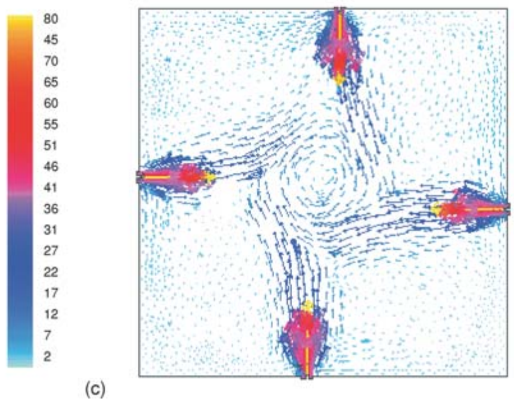

Figure 5. Samples of the flow pattern in TFF at the burners' level; (a) Contours of velocity magnitude (in m/s) in the TFF of the present study, (b) Contours of velocity magnitude (in m/s) in the TFF of [10]; (c) Velocity vectors in the TFF of [9]
(for color image see journal web site)

As shown in fig. 6, the jet remains intact and straight up to $y/L = 0.321$. Then it deflects up to $y/L = 0.464$ and finally continues its way in a straight line parallel to the symmetry axis of the coaxial nozzles up to $y/L = 0.500$.

The trajectory of the jet flowing in the positive direction of the y axis can be approximated by a third-order polynomial in the interval $0.321 < y/L < 0.464$ as:

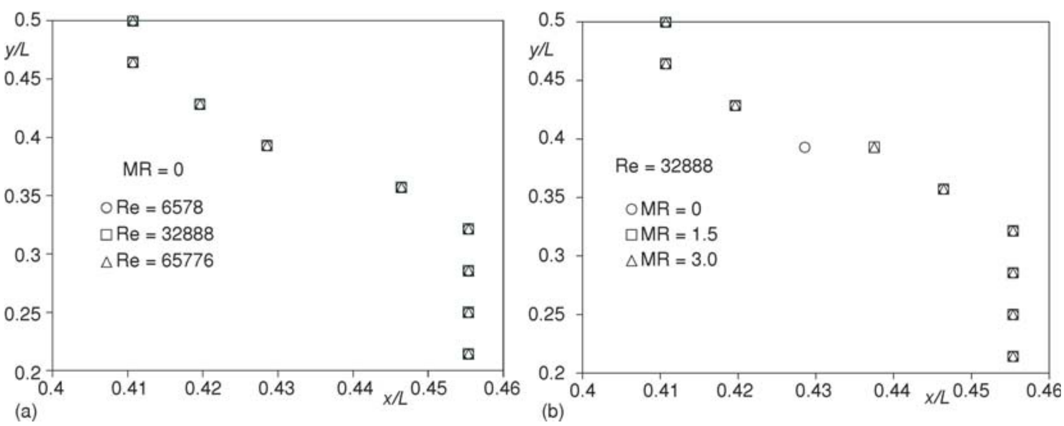

Figure 6. The trajectory of the coaxial fuel-air jets in the flow field of TFF; (a) at different Reynolds numbers, (b) at different momentum ratios

$$\frac{1}{L}\left(x-\frac{1}{2}(L-d_{\text{imag}})\right)=c_3'\left(\frac{y}{L}\right)^3+c_2'\left(\frac{y}{L}\right)^2+c_1'\left(\frac{y}{L}\right)+c_0' \tag{3}$$

where $c_0' = 1.6959$, $c_1' = 13.7179$, $c_2' = -36.1122$, and $c_3' = 30.6407$. This is shown in fig. 7. As suggested by Romadin [15], the imaginary circle diameter, see fig. 1(b), d_{imag} in eq. (3) is adjusted to be $0.089L$.

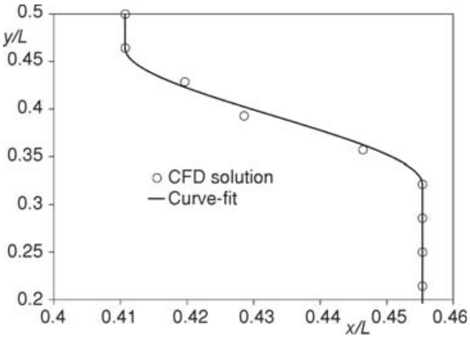

Figure 7. Least-squares curve-fit for the trajectory of the coaxial fuel-air jets

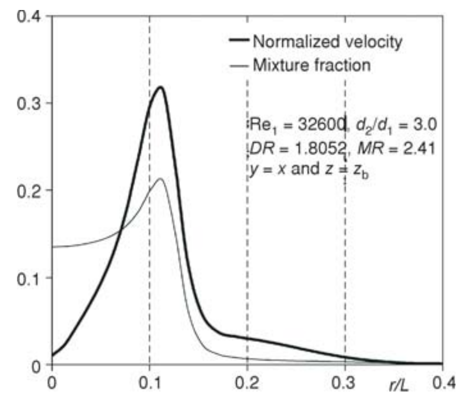

Figure 8. Position of the local maximums for velocity magnitude and mixture fraction in the vortex-dominated region

It can be seen from fig. 7 that the length of the intact part of the coaxial fuel-air jets before deflection is about $0.3L$. In other words, the coaxial fuel-air jets remain unaffected and free (straight) up to about $0.3L$ from the fuel nozzle exit. This implies that the effective radius of the large vortex in the middle of the furnace is:

$$r_{\text{vortex}} = (05 - 0.3)L = 0.2L \tag{4}$$

The effective radius of the r_{vortex} shows the distance from the vertical line passing through the furnace center ($r = 0$), within which the coaxial fuel-air jets are affected. The corresponding region limited by $r = r_{\text{vortex}}$ is called the vortex-dominated region. In this region, there are local maximums for velocity and concentration midway between $r = 0$ and $r = r_{\text{vortex}}$, at $r = r_{\text{peak}}$. According to the CFD simulations, r_{peak} is approximately $0.1L$. As a sample, distribution of the velocity magnitude and mixture fraction along the furnace diagonal $y = x$ at the burners' level is shown in fig. 8. In this figure, DR is the density ratio, *i. e.* the ratio of the ambient fluid (air) density to the round jet fluid (fuel) density.

As mentioned earlier, the calculated velocity and concentration fields should be corrected for the effect of the central vortex. According to the CFD simulations, x- and y-velocity components are to be corrected by multiplying with κ_1:

$$v_{\text{x,corr}} = \kappa_1 v_{\text{x}} \tag{5a}$$

$$v_{\text{y,corr}} = \kappa_1 v_{\text{y}} \tag{5b}$$

where $v_{\text{x,corr}}$ and $v_{\text{y,corr}}$ are corrected x- and y-velocity components and κ_1 is a second order polynomial as:

$$\kappa_1 = -\left(\frac{1}{r_{\text{peak}}^2}\right)r^2 + \left(\frac{2}{r_{\text{peak}}}\right)r \tag{6}$$

Such a correction causes the x- and y-velocities to become zero at the furnace center. This is theoretically true since the vortex in the middle of the furnace is a forced vortex.

In addition, the large central vortex entrains lean and rich zones and blends them together. The vortex ensures an efficient mixing of fuel with air and reduces the mixture fraction values, especially in the central (vortex-dominated) region of the furnace. According to the CFD simulations, the following correction takes account of the effect of the vortex on the concentration field:

$$f_{\text{ult}} = f^{\kappa_2} \tag{7}$$

In the above equation, f_{ult} is the ultimate mixture fraction and $\kappa_2 = 1.42$.

A computer program is developed in Matlab 7.1 to implement the new model. The program has a user-friendly structure and is kept as simple as possible. Thus future changes and improvements can easily be made. Here, an example of the extended model predictions is presented and compared with the results of the CFD solutions. In the example, the furnace dimensions and the details of the coaxial nozzles are the same as in fig. 1. Methane enters the furnace chamber from the four round fuel nozzles at a uniform velocity of 50.0 m/s and air is admitted through the annular air passages at 20.4 m/s. The Reynolds number based on the inner (fuel) jet parameters is 32600, the outer-to-inner pipe (nozzle) diameter ratio is 3.0, air-to-fuel density ratio is 1.8 and the outer-to-inner jet momentum ratio is 2.4.

Figure 9 shows contour lines of the dimensionless velocity at the burners' level. The x- and y-co-ordinates are normalized by the side length of the furnace square cross-section L and velocity is normalized by the velocity at the fuel nozzle exit.

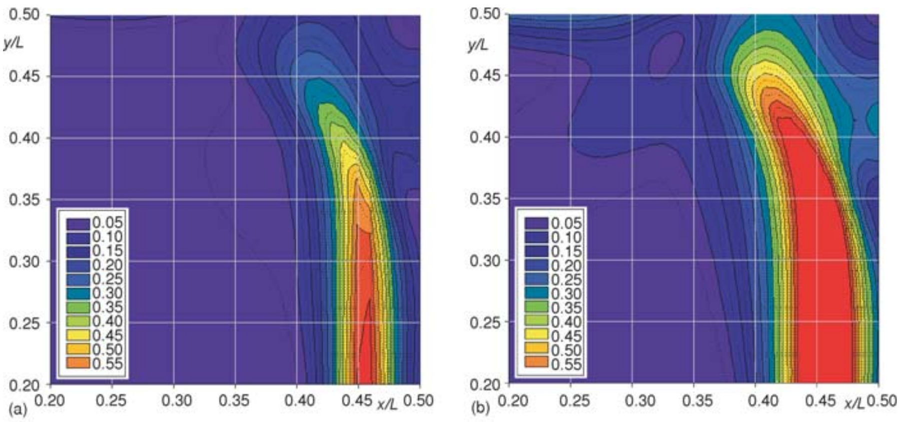

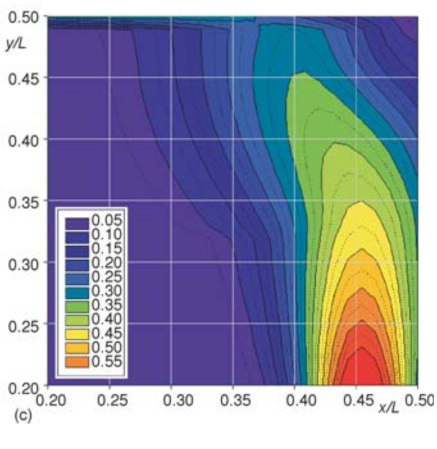

Figure 9. Contour lines of the normalized velocity at the burners' level; (a) The species transport model, (b) The conserved scalar model, (c) The new model
(for color image see journal web site)

The contour lines in figs. 9(a) and 9(b) are obtained from CFD solutions using the species transport model and the conserved scalar model, respectively. Contour lines in fig. 9(c) are predicted by the new model. It should be noted that each CFD solution requires about 600 minutes (10 hours), on average, to converge while the new model predicts the flow and concentration fields in only 1 minute.

Contour lines of the mixture fraction at the burners' level are shown in fig. 10. Again, the species transport model and the conserved scalar model are used to obtain the contour lines in figs. 10(a) and 10(b), respectively. The contour lines in fig. 10(c) are predicted by the new model in only 1 minute which is less than 0.2% of the time required by the CFD solutions (both the species transport model and the conserved scalar model) to converge.

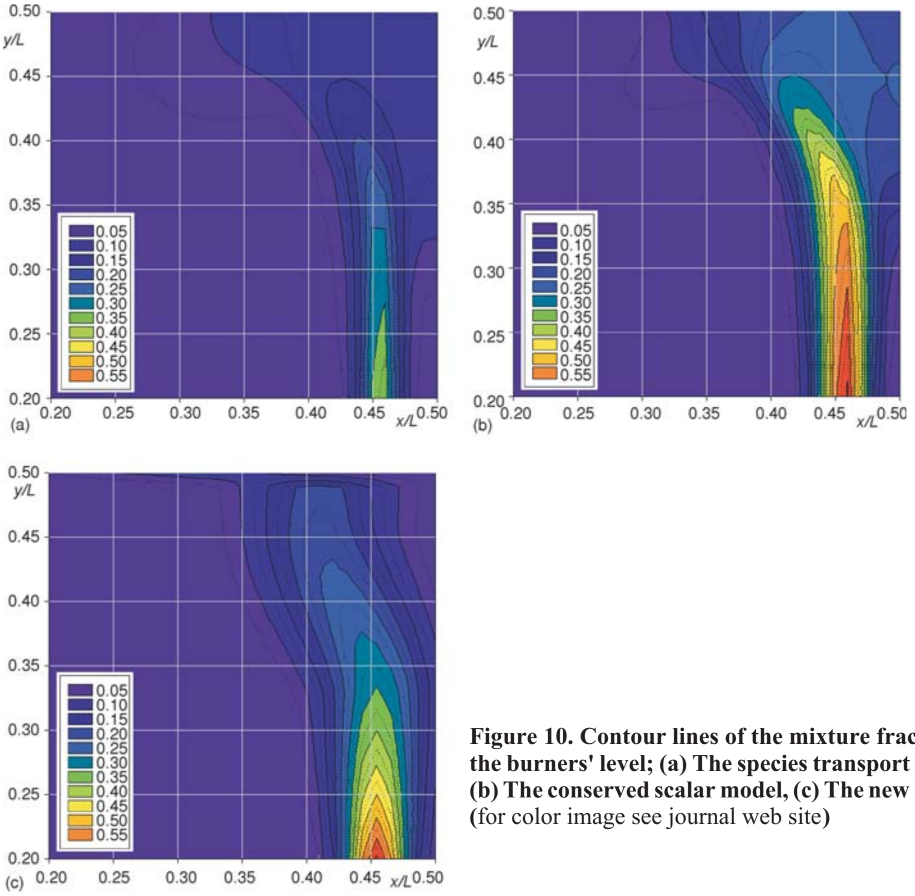

Figure 10. Contour lines of the mixture fraction at the burners' level; (a) The species transport model, (b) The conserved scalar model, (c) The new model (for color image see journal web site**)**

According to figs. 9 and 10, the flow and concentration fields predicted by the new model are in reasonable agreement with those obtained from the CFD solutions. The observed difference between the contour plots might be expected since the flow pattern is very complex and the new model is inherently different from the two CFD models. Even the two CFD models do not provide the same result, despite their identical nature. In sum, the new extended model provides sufficiently accurate estimates of the flow and concentration fields in TFF for engineering applications, although additional validation of the model is desirable during further development.

Conclusions

In the present work, the semi-analytical model previously established by the authors for the prediction of the behavior of coaxial turbulent gaseous jets is extended to be used in TFF with square horizontal cross-sections and to form the flow and mixing sub-model of the future multi-zone model for the simulation of such TFF. A computer program is developed in Matlab 7.1 to implement the new model. The program has a user-friendly structure and is kept as simple as possible. Thus future changes and improvements can easily be made. CFD simulations are made to validate the results of the new model using the flow solver Fluent 6.2. In order to verify the CFD solution procedure, a turbulent round jet injected into cross flow is simulated. The calculated jet trajectory and velocity profile are compared with other experimental and numerical data and good agreement is observed. Results show that the new extended model can provide very fast and reasonable predictions of the flow and concentration fields in TFF, although additional validation of the model is desirable during further development. The time required by the new model is only 1 minute which is less than 0.2% of that required by the CFD solution to converge, in the cases studied.

References

[1] Vagner, A. A., Raising the Reliability, Efficiency, and Ecological Safety of Operation of the BKZ-210-140F Boiler Transferred to Stage Firing of Kuznetsk Coal in a U-Shape Flame, *Power Technology and Engineering, 38* (2004), 3, pp. 159-163
[2] Habib, M. A., *et al*., Flow Field and Thermal Characteristics in a Model of a Tangentially Fired Furnace under Different Conditions of Burner Tripping, *Heat Mass Transfer, 41* (2005), 10, pp. 909-920
[3] Belosevic, S., *et al*., Three-Dimensional Modeling of Utility Boiler Pulverized Coal Tangentially Fired Furnace, *International Journal of Heat and Mass Transfer, 49* (2006), 19-20, pp. 3371-3378
[4] Diez, L. I., *et al.*, Numerical Investigation of NO_x Emissions from a Tangentially-Fired Utility Boiler under Conventional and Overfire Air Operation, *Fuel, 87* (2008), 7, pp. 1259-1269
[5] Li, S., *et al*., NO_x Emission and Thermal Efficiency of a 300 MWe Utility Boiler Retrofitted by Air Staging, *Applied Energy, 86* (2009), 9, pp. 1797-1803
[6] Zhou, Y., *et al*., Experimental and Numerical Study on the Flow Field in Upper Furnace for Large Scale Tangentially Fired Boilers, *Applied Thermal Engineering, 29* (2009), 4, pp. 732-739
[7] Modlinski, N., Computational Modeling of a Utility Boiler Tangentially-Fired Furnace Retrofitted with Swirl Burners, *Fuel Processing Technology, 91* (2010), 11, pp. 1601-1608
[8] Lotfiani, A., *et al.*, A Semi-Analytical Model for the Prediction of the Behavior of Turbulent Coaxial Gaseous Jets, *Thermal Science, 17* (2013), 4, pp. 1221-1232
[9] Khalilarya, Sh., Lotfiani, A., Determination of Flow Pattern and its Effect on NOx Emission in a Tangentially Fired Single Chamber Square Furnace, *Thermal Science, 14* (2010), 2, pp. 493-503
[10] Lotfiani, A., *et al*., Comparison of Flow and Mixing in a Gas-Fired Furnace in Tangential and Opposed Injection Modes, *Proceedings*, 20th Annual International Conference on Mechanical Engineering-ISME2012, Shiraz, Iran, 2012, p. 46
[11] Kamotani, Y., Greber, I., Experiments on a Turbulent Jet in a Cross Flow, *AIAA Journal, 10* (1972), 11, pp. 1425-1429
[12] ***, Fluent 6.2 User's Guide, Fluent Inc., Lebanon, N. H., USA, 2005
[13] Crabb, D., *et al.*, A Round Jet Normal to a Crossflow, *Journal of Fluids Engineering, 103* (1981), 4, pp. 568-580
[14] Majander, P., Siikonen, T., Large-Eddy Simulation of a Round Jet in a Cross-flow, *International Journal of Heat and Fluid Flow, 27* (2006), 3, pp. 402-415
[15] Romadin, V. P., Furnaces with Corner Firing Tangential Burners, *Thermal Engineering, 20* (1974), 7, pp. 79-89

Paper submitted: November 17, 2012
Paper revised: January 15, 2013
Paper accepted: January 28, 2013